

# Robust Semi-Blind Digital Image Watermarking Technique in DT-CWT Domain

Samira Mabtoul, Elhassan Ibn Elhaj, and Driss Aboutajdine

*Abstract*—In this paper a new robust digital image watermarking algorithm based on the Complex Wavelet Transform is proposed. This technique embeds different parts of a watermark into different blocks of an image under the complex wavelet domain. To increase security of the method, two chaotic maps are employed, one map is used to determine the blocks of the host image for watermark embedding, and another map is used to encrypt the watermark image. Simulation results are presented to demonstrate the effectiveness of the proposed algorithm.

*Keywords*—Image watermarking, Chaotic map, DT-CWT.

## I. INTRODUCTION

WITH the fast growth development of computer network technique and multimedia technology, digital media (such as image, video, audio or text) are stored, transmitted and distributed through Internet without any loss in the quality of the content. Hence, some way of protection of copyrighted digital data is required. A digital watermarking technique has been developed to protect intellectual property from illegal duplication and manipulation. Digital watermarking means embedding information into digital media in such way that it is imperceptible to a human observer but easily detected by means of computing operations in order to make assertions about the data. The watermark is needed to be robust against intentional removal by malicious parties. Thus by means of watermarking, the data is still accessible but permanently marked [1], [2].

Watermarking schemes can be robust or fragile. Robust watermarks are designed to resist to malicious or intentional distortions, such as general image processing and geometric distortions [3]; while a fragile watermarks are required for the purpose of authentication and verification. We can also classify watermarking schemes according to operation domain: the spatial domain and frequency domain. The simplest watermarking technique embeds a watermark directly into the spatial domain by modifying the Least Significant Bit (LSB) plane of the original image [4]. The watermarking scheme based on the frequency domains can be further classified into the Discrete Cosine Transform (DCT) [5], Discrete Fourier Transform (DFT) [6], Discrete Wavelet Transform (DWT) [7], Dual tree complex wavelet transform (DT-CWT) and others. In general, the transform domain techniques have provided more advantages and better performances than those of spatial ones in most of digital watermarking development and researches.

S. Mabtoul and D. Aboutajdine are with LRIT-GSCM, University Mohamed V, Rabat, Morocco, e-mail: mabtoul.samira@gmail.com.

E. Elhaj is with National Institute of Post and Telecommunications, Rabat, Morocco

The standard discrete wavelet transform has been exploited with great success across the scope of signal and image processing applications. For example, the DWT has the following advantages, such as good energy packing, perfect reconstruction with short support filters, no redundancy and low computation complexity. However, it lacks shift invariance (i.e., which means that small shifts in the input signal can cause major variations in the distribution of energy between DWT coefficients at different scales), and suffers from poor directional selectivity for diagonal features, because the wavelet filters are separable and real. In order to overcome these problems, complex wavelets have been proposed. Kingsbury's dual-tree complex wavelet transform (DT-CWT) is an outstanding example [8], [9]. The dual-tree complex wavelet transform is a relatively new development to the discrete wavelet transform (DWT), with important additional properties [9]:

- Approximate shift invariance;
- Good directional selectivity in 2-dimensions (2-D) with Gabor like filters (also true for higher dimensionality, m-D);
- Perfect reconstruction using short linear-phase filters;
- Limited redundancy (2:1 in 1-D and 4:1 in 2-D);
- Low computation comparing to other shift invariant transformations.

The work discussed in this paper is concerned with the design of robust and semi-blind watermarking algorithms with complex wavelet transform. We choose to use the complex wavelet transform as our watermarking domain because it is a relatively new transform and has useful properties for image processing applications. Previous work shows that DT-CWT gives good performance in image watermarking. In [10], [11], [12], [13], [14], [15], [16].

The outline of this paper is as follows: in the next section, we present the different steps for the proposed scheme. In Section III, we present the experimental results, and finally the paper is ended by a conclusion in Section IV.

## II. PROPOSED WATERMARKING ALGORITHM

The new watermarking method that we propose is based on dual-tree complex wavelet transform. The overview of our watermarking scheme is illustrated in Fig. 1. In this scheme, an input gray-scale image (512x512 pixels) is split into many non-overlapping small blocks with 8x8 pixels; the sub-image (256x256 pixels) is then constructed under control of secret key "key1". On the other hand, a watermark is encrypted and decomposed into different parts which are adaptively spread

spectrum and embedded in corresponding highest sub-bands of the 3-level DT-CWT transformed original sub-image. One example of oriented sub-bands of 3-level DT-CWT decomposition of an image is presented on Fig. 2.

This newly proposed scheme consists of four parts, including: image preprocess, watermark preprocess, watermark embedding, and watermark detection. Details are described in the following sections.

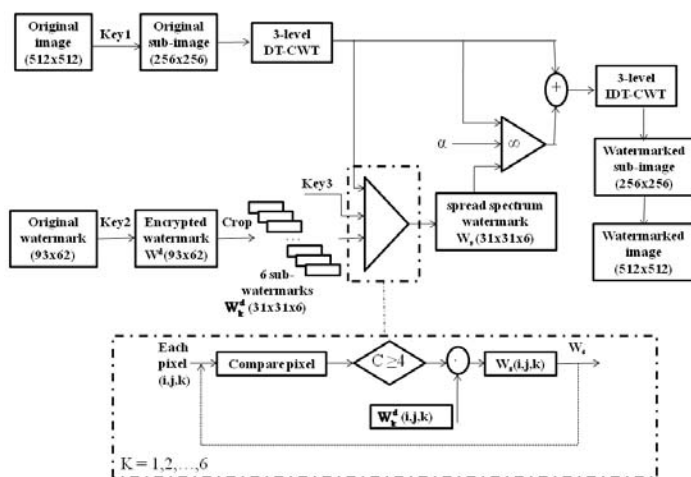


Fig. 1. Overview of the watermarking process.

- 2) We label the small blocks from number 1 to number 4096, then we generate a sequence  $S_i$ , which contains 4096 elements, by using the logistic map under a special initial value "Key1". The logistic map is one of the simplest chaotic maps, described by:

$$S_{k+1} = \mu S_k(1 - S_k); (k = 0, 1, 2, \dots); \quad (1)$$

where  $0 \leq \mu \leq 4$ . When  $3.5699456 \leq \mu \leq 4$ , the map is in the chaotic state.

- 3) We multiply each element of  $S_i$  by 4096 and then round it toward infinity. Therefore, we obtain a new sequence  $S_n$ , in the integer domain [1, 4096].
- 4) We select the forefront 1024 different elements in the new sequence noted by  $S_1$ , and we choose the small blocks accordingly. Finally, we construct the sub-image in a scanline order. Fig. 3 visualizes an example of this selection process.



Fig. 3. Example of a constructed sub-image.

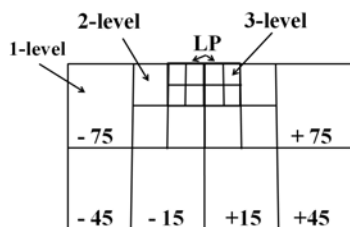


Fig. 2. 3-level DT-CWT decomposition of an image. LP corresponds to low-pass CWT coefficients.

### A. Image preprocess

In our watermark scheme, we apply the dual-tree complex wavelet transform only locally, we transform the sub-image, which is extracted from the host image, in the complex wavelet domain by using 3-level DT-CWT. Modifying coefficients at levels coarser than 3 tends to be relatively ineffective and to introduce visual artifacts.

To construct the sub-image, we use the following process [17]:

- 1) We first split the host image  $I_{orig}$ , into many non-overlapping small blocks with 8x8 pixels in a scanline order. With the image has 512x512 pixels, we will get 4096 small blocks.

### B. Watermark preprocess

In recent years, the chaotic data have been used for digital watermarking to increase the security. In our approach, a fast pseudo random number traversing method is used as the chaotic mechanism to change the watermark image  $W$ , which is a binary image  $\{-1, 1\}$  with 93x62 pixels, into a pseudo random matrix  $W^d$  by using the Eq. 2. Then the  $W^d$  is divided into small images with size 31x31 pixels, and totally 6 independent sub-watermarks are obtained  $W_k^d$  (Where  $k=1,2,\dots,6$ ).

$$Key2 : W \Rightarrow W^d, W^d(Key2(i, j)) = W(i, j); i, j \in N; \quad (2)$$

"Key2" presents the second key in our watermark procedure, which is an exclusive key to recreate the watermark image. Fig. 4 shows an example of encrypted watermark image and the result of sub-watermarks.

### C. Watermark embedding

Firstly, the original sub-image is decomposed by 3-level DT-CWT to obtain the 6 high-pass sub-bands. The DT-CWT coefficients are denoted by  $I$ . Secondly, With the Key "Key3" the position of the 6 sub-watermarks is scrambled. Based on magnitudes of the 3-level DT-CWT high-pass coefficients, the sub-watermarks  $W_k^d$  are adaptively spread spectrum. For each

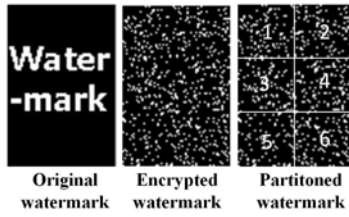


Fig. 4. The original watermark, the encrypted watermark, and the sub-watermarks.

pixel  $(i,j,k)$  of each highest frequency sub-band in  $\tilde{I}$ , the value is compared with those of its eight neighbors,  $t$  denotes the total number which the value is larger than its eight neighbors, as described by the following formula:

$$W_s(i, j, k) = \begin{cases} 1, & \text{if } (t \geq 4 \text{ and } W_k^d(i, j, k)=1) \text{ Or} \\ & (t < 4 \text{ and } W_k^d(i, j, k)= -1); \\ -1, & \text{else.} \end{cases} \quad (3)$$

The resultant spread spectrum watermark  $W_s$  is stored (i.e., used in the extraction process) and embedded into the 6 high-pass sub-band coefficients by using the following rule:

$$\hat{I}(i, j, k) = \tilde{I}(i, j, k) + \alpha * W_s(i, j, k) * |\tilde{I}(i, j, k)|; \quad (4)$$

where:  $k = 1, 2, \dots, 6$ .

- $\hat{I}$  : are the watermarked real parts of the DT-CWT coefficients.
- $\tilde{I}$  : are the original real parts of the DT-CWT coefficients.
- $W_s$ : is the spread spectrum watermark sequence.
- $\alpha$ : is an intensity parameter of image watermark.

By the inverse DT-CWT, the watermarked sub-image is obtained. Finally, according to the label sequence  $S_1$  (see sect. A), we put every small block of the watermarked sub-image into the original position of the host image. Thus, we get the watermarked image.

#### D. Watermark extracting

The extraction of watermark in image is an inverse process of embedding scheme. The watermark detection is accomplished without referring to the original image. Only the watermarked image, spread spectrum watermark  $W_s$ , and Keys (Key1, Key2, and Key3) need to be used. The watermark extraction algorithm can be summarized as follows:

- 1) The 3-level DT-CWT is performed on watermarked sub-image, which is extracted from the watermarked image using "Key1" (see sect. A).  $\hat{I}$  denotes the DT-CWT coefficients.
- 2) Constructed the encrypted watermark image  $\hat{W}_k^d$  : for each embed watermark pixel in  $\hat{I}$ , its value is compared with those of its eight neighbors;  $t'$  denotes the total number which the value of the pixel in  $\hat{I}$  is larger than its neighbors. Encrypted watermark image can be formed

as:

$$\hat{W}_k^d(i, j, k) = \begin{cases} 1, & \text{if } (t' \geq 4 \text{ and } W_s(i, j, k)=1) \text{ Or} \\ & (t' < 4 \text{ and } W_s(i, j, k)= -1); \\ -1, & \text{else.} \end{cases} \quad (5)$$

- 3) Reconstructed watermark image  $\hat{W}$  : the 6 parts of the watermark  $\hat{W}_k^d$  are collected under control of secret key "key3", then the original large watermark image  $\hat{W}$  can be reconstructed by using the inverse transform of the preprocessing with the secret key "Key2".

This can be shown in Fig. 5, where the original image, the watermarked image, the absolute difference between the original and the watermarked images, the 6 parts of spread spectrum watermark, the 6 parts of extracted encrypted watermark and the reconstructed watermarks with true and false keys. Moreover, if one secret key is changed, the final watermark can not still survive.

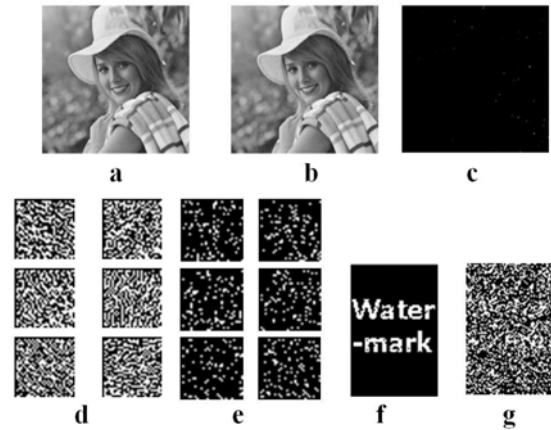


Fig. 5. An example of the mentioned watermark extracting procedure. (a) original image, (b) watermarked image, (c) absolute difference between the original image and the watermarked image, (d) the 6 parts of spread spectrum watermark, (e) the 6 parts of extracted encrypted watermark, and (f)-(g) the reconstructed watermarks with true and false keys, respectively.

### III. EXPERIMENTAL RESULTS

To evaluate the effectiveness of the proposed approach, four standard grayscale images are used, Lena image (512x512), Zelda image (512x512), Baboon image (512x512), and Elaine image (512x512). The embedded watermark is a binary image with the size of (93x62) pixels. In all our experiments, we chose watermark intensity parameter  $\alpha = 0.02$  to guarantee high fidelity.

We choose to compare our scheme in DT-CWT domain with the scheme presented in [18]. When a new watermarking algorithm combining DWT and DCT is proposed.

1) *The quality of watermarked images*: In this work, we use peak singular-to-noise ratio (PSNR) to measure the quality of watermarked images. It is defined as:

$$PSNR(I, \hat{I}) = 20 * \log\left(\frac{255}{\frac{1}{M*N} \sum_i \sum_j [I(i, j) - \hat{I}(i, j)]^2}\right); \quad (6)$$

Where  $I$  is the original image and  $\hat{I}$  is the watermarked version, both with dimensions  $M \times N$ .

From table 1, we can see that the proposed scheme is better than the scheme presented in [18] in terms of the imperceptibility.

TABLE I  
 PSNR BETWEEN ORIGINAL IMAGE AND WATERMARKED IMAGE (DB)

images	Proposed Scheme	Scheme in [18]
Lena	76.1884	41.6333
Zelda	87.0014	39.2513
Baboon	86.2956	41.5832
Elain	80.9490	41.7581

2) *Robustness to various attacks*: The robustness of the proposed watermarking scheme is measured by the similarity metric between the detected watermark  $\hat{W}$  and the original watermark  $W$ , which is defined as:

$$Sim(\hat{W}, W) = \frac{\sum_i \sum_j (\hat{W}(i, j) \cdot W(i, j))}{\sum_i \sum_j (W^2(i, j))}; \quad (7)$$

Simulations results for common signal processing attacks such as salt & pepper noise, gaussian noise, JPEG compression and median filter are performed and compared with the results of [18]. Experiment results are shown in tables II - V. A comparison of different results indicates the high efficiency of our proposed approach compared to scheme [18].

We also evaluate our approach by StirMark 4.0 [19]. The results for test images are shown in table VI. It can be seen that our algorithm can successfully resist JPEG compression, Median filter, Scaling, Affine, Remove lines, and PSNR attacks.

Some examples of attacked watermarked Zelda and the corresponding extracted watermark are shown in Fig. 6.

TABLE II  
 THE VALUE SIM AFTER ADDING SALT & PEPPER NOISE INTO WATERMARKED IMAGE

images	Salt & Pepper Noise					
	Proposed Scheme			Scheme in [18]		
	Noise density			Noise density		
	0.002	0.003	0.005	0.002	0.003	0.005
Lena	0.9329	0.9240	0.9121	0.9173	0.9037	0.8445
Zelda	0.9270	0.9195	0.9001	0.8571	0.8265	0.7932
Baboon	0.9210	0.9240	0.9180	0.9460	0.8990	0.8368
Elain	0.9210	0.9151	0.9106	0.9474	0.8661	0.8548

#### IV. CONCLUSION

Proposed method describes robust and semi-blind digital image watermarking in frequency domain, which is computationally efficient. This method applies the Dual Tree Complex Wavelet Transform; the watermark image is encrypted and decomposed into different parts which are adaptively spread spectrum and added into the DT-CWT coefficients. The experimental results have confirmed that this new scheme has high fidelity and it is robust against JPEG compression, Scaling,

TABLE III  
 THE VALUE SIM AFTER ADDING GAUSSIAN NOISE INTO WATERMARKED IMAGE

images	Gaussian noise insertion					
	Proposed Scheme			Scheme in [18]		
	Variance			Variance		
	0.002	0.003	0.005	0.002	0.003	0.005
Lena	0.8718	0.8584	0.8689	0.7936	0.7485	0.6668
Zelda	0.8480	0.8584	0.8495	0.7946	0.7781	0.6880
Baboon	0.8554	0.8510	0.8316	0.7929	0.7381	0.7339
Elain	0.8465	0.8331	0.8420	0.8693	0.8476	0.7555

TABLE IV  
 THE VALUE SIM AFTER WATERMARKED IMAGE JPEG COMPRESSED

images	JPEG compression					
	Proposed Scheme			Scheme in [18]		
	Quality factor			Quality factor		
	75 %	60 %	40 %	75 %	60 %	40 %
Lena	0.9359	0.9314	0.9329	0.8612	0.8085	0.6916
Zelda	0.9329	0.9270	0.9240	0.8640	0.8252	0.7000
Baboon	0.9329	0.9255	0.9240	0.8529	0.7788	0.6562
Elain	0.9374	0.9285	0.9255	0.8577	0.8156	0.6967

TABLE V  
 THE VALUE SIM AFTER MEDIAN FILTER

images	Median filter	
	Proposed Scheme	Scheme in [18]
	Median filter(3x3)	Median filter(3x3)
Lena	0.9285	0.7330
Zelda	0.9300	0.8132
Baboon	0.8957	0.5941
Elain	0.9165	0.7771

Affine, Remove lines, PSNR attacks, and signal processing (Salt & pepper, Gaussian noise, and Median filter). The comparison of the proposed scheme [18] shows that our DT-CWT approach is more effective.

#### REFERENCES

- [1] Juergen Seitz. "Digital Watermarking For Digital Media", Information Resources Press Arlington, VA, USA, ISBN 159140519X, 2005.
- [2] Chun-Shien Lu. "Multimedia Security: Steganography and Digital Watermarking Techniques for Protection of Intellectual Property", Idea Group Publishing, London, ISBN 1591401925, 2004.
- [3] J.L. Dugelay, S. Roche, C. Rey, G. Dorr, "Still image watermarking robust to local geometric distortions". IEEE transactions on image processing, 2006, 15 N9, 2831-2842.
- [4] L. O'Gorman, H. Berghel. "Protecting Ownership Rights through Digital Watermarking". IEEE Computer 1996, 29, 101-103.
- [5] J. R. Hernandez, M. Amado, F. Prez-Gonzlez. "DCT-domain watermarking techniques for still images: Detector performance analysis and a new structure". IEEE Trans. on Image Processing 2000, Special Issue on Image and Video Processing for Digital Libraries, 9(1), 55-68.
- [6] J. Kusyk, A. M. Eskicioglu. "A Semi-blind Logo Watermarking Scheme for Color Images by Comparison and Modification by Comparison and Modification of DFT Coefficients". Optics East 2005, Multimedia Systems and Applications VIII Conference 2004, 23-26.
- [7] M. Barni, F. Bartolini, A. Piva. "Improved Wavelet based Watermarking Through Pixel-Wise Masking". IEEE Transactions on Image Processing 2001, 10, 783-791.

TABLE VI  
 TEST RESULTS WITH STIRMARK 4.0

StirMark Attacks	Lena	Zelda	Baboon	Elain
JPEG__15	0.9165	0.8972	0.9076	0.9001
JPEG__30	0.9255	0.9195	0.9165	0.9225
JPEG__50	0.9359	0.9195	0.9240	0.9300
JPEG__80	0.9389	0.9314	0.9404	0.9389
MEDIAN__5	0.9106	0.9225	0.8784	0.9121
MEDIAN__7	0.9016	0.9001	0.8450	0.9121
MEDIAN__9	0.8852	0.8823	0.7973	0.9016
RESC__50	0.9329	0.9314	0.9334	0.9255
RESC__75	0.9344	0.9344	0.9195	0.9195
RESC__90	0.9121	0.9091	0.8763	0.9151
RESC__50	0.9210	0.9255	0.9240	0.9255
AFFINE__1	0.8748	0.8689	0.7809	0.8227
AFFINE__2	0.7809	0.7660	0.6572	0.6602
AFFINE__5	0.7809	0.8018	0.7258	0.7422
AFFINE__8	0.8077	0.8227	0.7481	0.7556
RML__20	0.9121	0.9046	0.8942	0.9046
RML__40	0.9165	0.9106	0.8823	0.9001
RML__100	0.9255	0.9195	0.8793	0.9195
PSNR__10	0.9491	0.9434	0.9434	0.9434
PSNR__30	0.9491	0.9434	0.9434	0.9434
PSNR__60	0.9491	0.9434	0.9434	0.9434

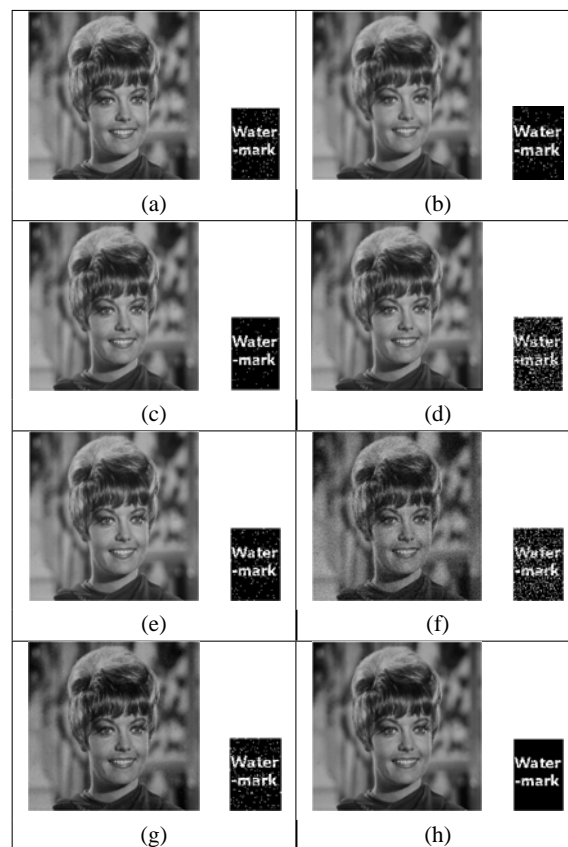


Fig. 6. The effect of attacks on watermarked "Zelda". (a) JPEG compressed watermarked image of quality 30%, (b) Median filtered watermarked image under factor 5, (c) Scaled Watermarked image (ratio 75%), (d) Watermarked image under affine attack, (e) Removed 100 lines of the watermarked image, (f) Watermarked image after adding gaussian noise (variance : 0.002), (g) Watermarked image after adding Salt & pepper noise (noise density : 0.005) and (h) Watermarked image with 40% of PSNR quality with the corresponding detected watermark images.

editors, proceedings of electronic imaging, security and watermarking of multimedia contents III 2001, 4314.

[8] N.G. Kingsbury, "Complex wavelets for shift invariant analysis and filtering of signals". Journal of Applied and Computational Harmonic Analysis, vol. 10, no. 3, pp. 234253, May 2001.

[9] I.W. Selesnick, R.G. Baraniuk and N.G. Kingsbury, "The Dual-Tree Complex Wavelet Transform". IEEE Signal Processing Magazine, vol. 22, no. 6, pp. 123151, Nov. 2005.

[10] P. Loo, N. G. Kingsbury. "Watermarking using complex wavelets with resistance to geometric distortion", Proceedings Proceeding of the European Signal Processing Conference, EUSIPCO 2000, 5-8, 2000.

[11] H. Yongjian, J. Huang, S. Kwong, Y. Chan. "Image Fusion Based Visible Watermarking Using Dual-Tree Complex Wavelet Transform", Computer Science, Digital Watermarking: Second International Workshop, IWDW 2003, 2939/2004, 86-100.

[12] S. Mabtoul, E. Ibn-Elhaj, D. Aboutajdine, "A Robust Digital Image Watermarking Method Using Dual Tree Complex Wavelet Transform". The Thirteenth IEEE Symposium on Computers and Communications (ISCC'08) July 6-9, 2008, Marrakech, Morocco.

[13] S. Mabtoul, E. Ibn-Elhaj, D. Aboutajdine, "A BLIND CHAOS-BASED COMPLEX WAVELET-DOMAIN IMAGE WATERMARKING TECHNIQUE". Journal IJCSNS, VOL.6 No.3, pp. 134-139, March 2006.

[14] L. Joong-Jae, W. Kim, L. Na-Young, G. Kim. "A New Incremental Watermarking Based on Dual-Tree Complex Wavelet Transform", Journal of the Supercomputing 2005, 33(1-2), 133-140.

[15] N. Terzija and W. Geisselhardt, "Digital image watermarking using Complex Wavelet Transform," in Proc. of ACM Workshop on Multimedia and Security, 2004, pp. 193198.

[16] L. E. Coria, M. R. Pickering, P. Nasiopoulos, and R. K. Ward, "A video watermarking scheme based on the Dual-Tree Complex Wavelet Transform," IEEE Transactions on Information Forensics and Security, vol. 3, no. 3, pp. 466-474, 2008.

[17] Z. Dawei, C. Guanrong and L. Wenbo, "A chaos-based robust wavelet-domain watermarking algorithm", Chaos, Solitons and Fractals, Vol. 22, pp. 47-54, Oct. 2004.

[18] C. Jin, Z. Zhang, Y. Jiang, Z. Qu, C. Ma, "A Blind Watermarking Algorithm Based on Modular Arithmetic in the Frequency Domain". K. Elleithy (ed.), Advances and Innovations in Systems, Computing Sciences and Software Engineering, ISBN 978-1-4020-6263-6 (Print) 978-1-4020-6264-3 (Online), 543547. 2007.

[19] F. A. P. Petitcolas, M. Steinebach, F. Raynal, J. Dittmann, C. Fontaine, N. Fats. A public automated web-based evaluation service for watermarking schemes: StirMark Benchmark. In Ping Wah Wong and Edward J. Delp,